Front. Environ. Sci. Engin. China 2010, 4(1): 12–19
DOI 10.1007/s11783-010-0012-9

REVIEW ARTICLE

Review on the applications of Tropospheric Emissions Spectrometer to air-quality research: Perspectives for China

Yuxuan WANG (✉), Yuqiang ZHANG, Jiming HAO

Department of Environmental Science and Engineering, Tsinghua University, Beijing 100084, China

© Higher Education Press and Springer-Verlag Berlin Heidelberg 2010

Abstract The Tropospheric Emissions Spectrometer (TES) aboard the National Aeronautics and Space Administration's (NASA's) Aura satellite launched in July 2004 is the first satellite instrument to provide simultaneous retrievals of ozone (O_3) and carbon monoxide (CO) throughout the Earth's lower atmosphere. This paper briefly reviews the TES instrument, the retrieval of O_3 and CO profiles, and the validation of the retrievals. The applications of TES O_3 and CO products include mapping the vertical and horizontal distribution of tropospheric O_3 and CO and their correlations, examining the regional and continental outflow, and analyzing the variability of the two species associated with certain weather and climatic conditions, such as El Niño and the Asian monsoon. TES retrievals of O_3 and CO offer an important new source of satellite data over China with good spatial and temporal coverage that can provide evaluation and constraints on the performance of chemical transport models in simulating the general features of ozone pollution over China. Special observations have been conducted and requests may be submitted to the TES team to make geographically focused observations of O_3 and CO over China.

Keywords Tropospheric Emissions Spectrometer (TES), ozone, carbon monoxide, China

1 Introduction

Ozone is one of key species in the atmosphere. About 90% of the total ozone resides in the stratosphere, where it shields the Earth's surface from harmful UV radiation. The troposphere contains about 10% of the total ozone. Tropospheric ozone is produced by the photochemical oxidation of volatile organic carbons (VOCs) and CO in the presence of NO_x ($NO_x \equiv NO_2 + NO$). Downward transport of ozone from the stratosphere is a relatively smaller source of ozone in the troposphere. Photolysis of ozone in presence of water vapor is the primary source of hydroxyl radical (OH), which is the key oxidant in the troposphere. Reactions with OH are the principal sink for a large number of important species with implications for both the regional and global environment, including air pollutants and greenhouse gases [1]. In that sense, ozone is not only a greenhouse gas by itself; it also has an indirect effect on the concentrations of other greenhouse gases by affecting their lifetime with respect to oxidation by OH.

Ground-level ozone is the principal harmful component of photochemical smog. In contrast to stratospheric ozone depletion, tropospheric ozone has increased since the Industrial Revolution—especially in the Northern Hemisphere—as a consequence of human activity [2]. The implication of this increase on the chemical and radiative budget of the global atmosphere depends largely on its altitude. It is very important, therefore, to map the global three-dimensional distribution of tropospheric ozone and its precursors in order to improve our understanding of the factors controlling ozone in different regions of the troposphere.

Ozone has a lifetime of several days in the continental boundary layer, but weeks in the free troposphere [3–5], and thus can be regarded as a global pollutant. Strict control measures on ozone and its precursors have been adopted in North America and some European countries. Emissions of ozone precursors were projected to continue the current path of rapid increases in Asia, especially in China, the world's fastest growing economy [6,7]. Ozone profiles recorded over Beijing by the MOZAIC aircraft data from 1995 to 2005 suggested that ozone in the lower troposphere over Beijing had a strong trend of increase, at approximately 2% per year [8]. Observations of surface ozone at a coastal site in Hong Kong from 1994 to 2007 suggested that the rate of increase was 0.58 ppbv/y at the

Received October 14, 2009; accepted November 11, 2009

E-mail: yxw@tsinghua.edu.cn

site. In comparison, the means between years 2001–2007 yielded a higher rate of increase at 0.87 ppbv/y for a 7-year period [9].

Increasing ozone concentration in the lower troposphere in China is a matter of great concern; however, scientific measurements of surface ozone and tropospheric ozone profiles have been sparse in China. The literature reported only a few surface ozone measurements in China, such as Shangdianzi [10] and Miyun [11] in North China Plain and Lin An in Yangtze River Delta [12]. Satellite remote sensing of air quality has evolved dramatically over the last decade and can provide simultaneous observations of many atmospheric gaseous and particulate species on a large scale, complementing the ground air quality monitoring network. Tropospheric Emissions Spectrometer (TES) is one of four science instruments aboard the National Aeronautics and Space Administration's (NASA's) EOS Aura satellite, which was launched on July 15, 2004. The satellite flies at an altitude of 705 km (438 miles) in a near-Polar, Sun-synchronous orbit. The spacecraft advances 22° westward in each orbit, and the orbital pattern repeats every 233 orbits (16 d). The satellite daytime overpass over Beijing is approximately at 15:00 local time. TES standard retrieval products include vertically resolved profiles for ozone, carbon monoxide, water vapor, deuterated water vapor, and methane. TES is the first satellite instrument to provide simultaneous retrieval of carbon monoxide (CO) and ozone (O_3).

In this review, we first briefly introduce the TES instrument and the retrieval and the validation of the TES CO and O_3 products. The current applications of TES data in air quality monitoring will be discussed in Section 3, followed by the perspective of the feasibility and restrictions for the applications of TES products in China.

2 TES instrument and retrieval

2.1 Instrument and viewing geometry

TES is a Fourier Transfer Infrared Spectrometer (FTIR) with spectral coverage of 650 to 3050 cm^{-1} (3.3–15.4 μm) at a spectral resolution of 0.1 cm^{-1} (low resolution at nadir) or 0.025 cm^{-1} (high resolution at limb). Along the viewing path of the TES instrument, the spectral dependent attenuations of the radiance either due to the absorption or emission of the atmospheric species are captured by TES. The high spectral resolution allows the radiance signals to capture the vertical information in temperature, pressure, and the species distribution. In most atmospheric conditions, TES ozone and CO nadir retrievals therefore provide more than one piece of information vertically in the troposphere. TES has both the nadir- and limb-viewing geometry. Advantages to the nadir-viewing geometry are the lower probability of cloud interference and a good horizontal spatial resolution. The main disadvantage to the nadir-viewing geometry is limited vertical resolution. TES uses the nadir-viewing geometry to measure temperature and the primary species (H_2O, HDO, O_3, CH_4, and CO). Advantages to the limb-viewing geometry are better vertical resolution and enhanced sensitivity to trace constituents. Disadvantages are the higher probability of cloud interference in the troposphere and the poorer line-of-sight spatial resolution. For TES, the horizontal resolution is 5 km × 8 km at nadir and 26 km × 41.8 km at limb. As of May 25, 2005, TES uses its limb-viewing geometry only during special observations [13].

2.2 Observation modes

TES has two basic operating modes: Global Survey (GS) and Special Observations (SO). Global Surveys are the routine observations of TES that are conducted every two days, producing the "standard product." Special Observations include all other measurements.

Global Surveys are made on roughly a "one day on, one day off" cycle for the main purpose of extending the instrument's lifetime. Figure 1 shows retrieved CO columns at observation geolocations in a global survey period in September 22–24, 2004 as an example. Special Observations are conducted only during the 'off' periods, including Stare, Transect, and Step & Stare mode, depending on the scientific requirements. Stare mode is used to point at a specific location for a longer time of up to 240 s, as long as the location is within ±45° of the nadir direction. Stare mode is used mainly for localized validation, volcano monitoring, and observations of biomass burning plumes. Transect mode is used to point at a set of contiguous areas to cover about 850 km in nadir mode. When in Step & Stare mode, TES points at a nadir location for 4 s and moves about 35 km forward to a new nadir location. Figure 2 illustrates column O_3 retrieved by TES for a specific Step & Stare and Transect orbit.

2.3 TES retrieval method

The TES retrieval uses the optimal estimation method [15,16]. The retrieval is the linear combination of the weighted *a priori* constraint and the true profile. The retrieved mixing ratio profile of a gas can be expressed as

$$x_{ret} = Ax + (I - A)x_a + G\varepsilon, \quad (1)$$

where x is the true vertical profile, and x_a is the a priori profile representing the knowledge about the species profile before the measurement is made. The x_a for TES is derived from monthly mean outputs of chemical transport model simulations [17]. A is the averaging kernel matrix, G is the retrieval gain (contribution function), ε is spectral measurement error, and I is the unit matrix. The averaging kernel matrix (A) represents the vertical sensitivity of a retrieved profile to the true profile. In the ideal case of a unity averaging kernel matrix, i.e., $A = I$, the

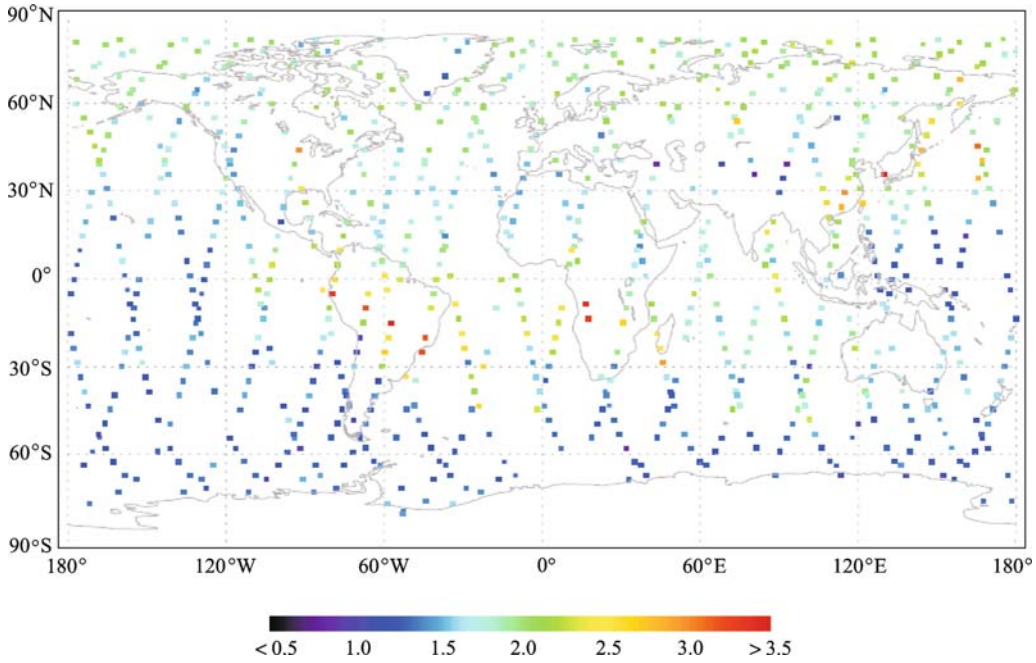

Fig. 1 TES total CO columns (colored coding; in unit of 10^{18} molecules·cm^{-2}) at observation geolocations with enlarged symbols in a global survey period in September 20–21, 2004
(data version 002; adapted from Luo et al. [14])

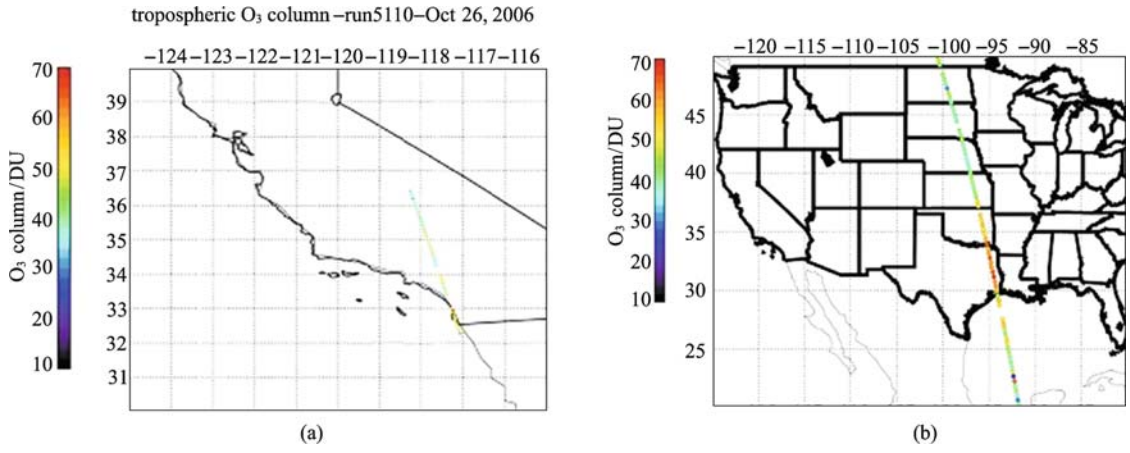

Fig. 2 TES different observation mode: Transect mode (a) and the Step & Stare (b)
Notes: the color lines represent the projection of the orbit on the surface; the color represents TES O_3 column in Dobson Unit in the observation period; a Dobson Unit is 2.69×10^{16} molecules·cm^{-2} (http://tes.jpl.nasa.gov/visualization/l2plots/, read on October 9, 2009)

retrieval profile x_{ret} would equal the true profile x plus the noise. However, in reality, the averaging kernels of current satellite instruments, such as TES, are far from unity. The averaging kernels are determined by the instrument characteristics, including the sensitivities of the measurements to the gas's concentration at different altitudes, the instrument's signal-to-noise ratio, and the a priori constraint. Another important parameter for the retrieval is the degree of freedom for signal (DOF). DOF presents the number of independent pieces of information on the vertical in the retrieved profile [16]. TES standard products (global surveys), consisting of 16 orbits of nadir vertical profiles obtained every other day, provide 2–3 pieces of information for ozone and 1–2 pieces of information for CO in the troposphere [14,18].

TES data processing includes four parts: level 1A (L1A), level 1B (L1B), level 2 (L2), and level 3 (L3). At L1A, the raw data from the spacecraft are collected, and the instrument outputs (called interferograms) are reconstructed. At L1B, the interferograms are phase-corrected,

Fourier transformed to spectra, radiometrically calibrated, and resampled onto a common frequency grid. Certain data quality flags are added at this juncture, and the results are passed to L2. At L2, vertical concentration profiles of the selected species are extracted from the data through the retrieval process discussed above. L3 uses the retrieved profiles from L2 and interpolates or averages them onto the global maps of daily and monthly time steps. The L3 data are useful browse products. TES data are available from the NASA website (http://eosweb.larc.nasa.gov/PRODOCS/tes/table_tes.html).

2.4 Validation of TES retrieval

The products of O_3 and CO retrievals from TES have been validated using measurements from other satellites, aircrafts, ozonesonde, and surface observations [14,18–21]. Nassar et al. [18] compared TES version 2 (V002) nadir ozone profiles with ozonesonde profiles from the Intercontinental Chemical Transport Experiment Ozonesonde Network Study (IONS), the World Ozone and Ultraviolet Data Center (WOUDC), the Global Monitoring Division of the Earth System Research Laboratory (GMD), and the Southern Hemisphere Additional Ozonesondes archives (SHADOZ). They found that TES O_3 retrieval has a positive bias ranging from 3.7 ppbv to 9.2 ppbv in the lower troposphere and from 2.9 ppbv to 10.6 ppbv in the upper troposphere, excluding the Arctic and Antarctic, where TES sensitivity is low.

Richards et al. [20] validated TES tropospheric ozone profiles using airborne differential absorption lidar (DIAL) profiles obtained during the Intercontinental Chemical Transport Experiment–B (INTEX-B) campaign from March–May 2006. The aircrafts conducted several flights designed to obtain DIAL ozone profile measurements over the United States, East Asia, and the Pacific that were spatially coincident with 243 Step & Stare special observations made by TES. The comparisons of TES and DIAL ozone profiles showed that, on the average, TES exhibits a small positive bias in the troposphere of 5%–15%, or about 7 ppbv. This is consistent with the bias reported by Nassar et al. [18].

Luo et al. [14] compared CO profiles retrieved from TES with that from the Measurements of Pollution in the Troposphere (MOPITT) instrument aboard the NASA Terra satellite. They suggested that the CO retrieval products of the two satellite instruments, in terms of vertical profiles and total columns, could not be compared directly because of different *a priori* profiles and averaging kernels used in the retrievals. Averaging kernels represent the instrument characteristics, while the *a priori* profiles are user defined inputs to the retrieval. After accounting for the influence of the two parameters on CO retrievals, Luo et al. [14] found good agreement with no systematic differences between the CO profiles and the columns from the two instruments.

3 Applications

Since the launch of TES in 2004, TES retrieval products of O_3 and CO have been used extensively to analyze the vertical and horizontal distributions of the two gases on regional and global scales. TES retrievals can be adopted to map the vertical profiles of tropospheric O_3 and CO, examine the regional and continental outflow of O_3 and CO, and analyze the variability of the two species resulting from certain weather and climatic conditions, such as El Niño and the Asian monsoon.

3.1 O_3-CO correlations from TES

TES is the first satellite to provide vertical information on tropospheric ozone with simultaneous measurements of CO on a global basis. CO is a relatively long-lived tracer of a variety of combustion sources (especially transportation and biomass burning). The O_3-CO correlation derived from the TES retrievals can be analyzed to understand the global anthropogenic influence on O_3. Zhang et al. [21] examined the global distribution of O_3-CO correlations derived from TES in the middle troposphere (618 hpa) for July 2005. In their study, TES data were gridded into 10×10 grids, each grid cell containing 20–60 pairs of TES O_3-CO data from which the correlation analysis were evaluated. Figure 3 summarizes the global distribution of O_3-CO correlation coefficients and d[O_3]/d[CO] enhancement ratio derived from TES for July 2005 by Zhang et al. [21]. Significant positive correlations (correlation coefficient $R > 0.4$) were observed downwind of the eastern United States and East Asia, and over Central Africa, regions that are already known to have strong production and export of O_3 in the northern hemispheric summer [22–24]. The d[O_3]/d[CO] enhancement ratio of 0.4–1.0 $mol \cdot mol^{-1}$ was derived over the polluted continents. The O_3-CO correlations from TES were also compared to correlations simulated by the GEOS-Chem global chemical transport model, for the purpose of cross-validations of both TES and the model. The GEOS-Chem model reproduced positive O_3-CO correlations over the same region as TES but with much stronger correlation coefficients and extending much further downwind of the continents than TES. Zhang et al. [21] suggested that the discrepancy was mainly caused by retrieval errors in the TES V001 data version adopted in their study. These errors have been corrected in the later TES data version (V002 and V003).

The correlations and enhancement ratio between O_3 and CO retrieved from TES can be used to analyze the continental outflow of ozone and the impact on air quality of downwind countries. Zhang et al. [25] integrated the TES retrieval and aircraft measurements during the INTEX-B campaign to qualify the transpacific transport of Asian pollution and its effect on surface ozone over North America. They found that TES O_3 and CO did not

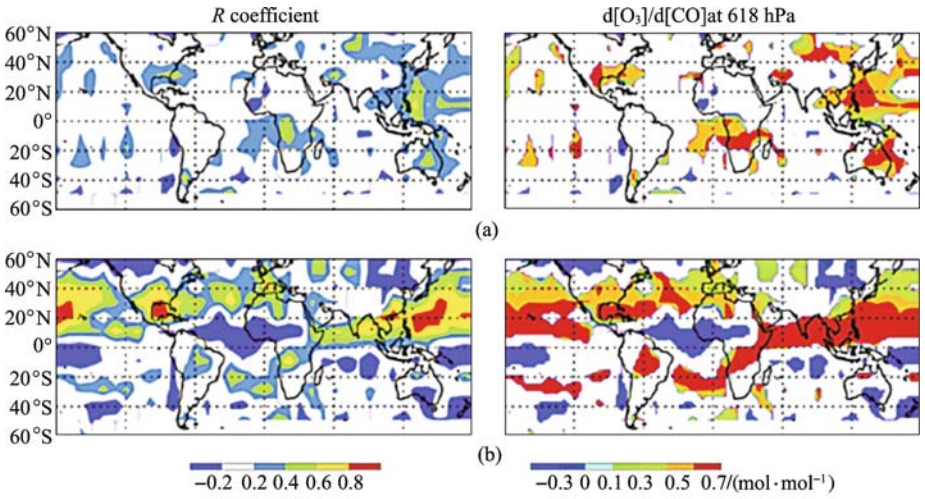

Fig. 3 O_3-CO correlations for July 2005 at 618 hPa from (a) TES, (b) GEOS-Chem with TES averaging kernels applied
Notes: the correlation coefficients R (left panels) and the linear regression slopes d[O_3]/d[CO] (right panels) are shown; white regions correspond to $|R| < 0.2$. (Adapted from Zhang et al. [21])

exhibit strong correlations over the North Pacific due to the stratospheric influence over the region. Removing this stratospheric influence reveals strong positive correlations between TES O_3 and CO, with the correlation coefficient exceeding 0.5 and becoming statistically significant at a 95% confidence interval. The correlations, likely driven by the contrast between Asian pollution outflow and clean tropical marine air masses, indicate collocated export of O_3 and CO pollution from Asia.

3.2 Variation of tropospheric ozone influenced by climatic phenomenon

TES provides a continuous record of annual data since it was launched in 2004 and offers an important opportunity to investigate the interannual variability in tropospheric ozone and CO over specific regions affected by certain climatic phenomena, such as El Niño and the Asian monsoon. Logan et al. [26] examined global TES data from October to December in 2005 and 2006 and found large differences in CO, O_3, and H_2O over Indonesia and the eastern Indian Ocean in the middle troposphere between the two years. In 2006, it was a moderate El Niño year, and it had the lowest rainfall over Indonesia since 1997. O_3 over the regions at the 511 hPa retrieval level from TES was higher by 15–30 ppb (30%–75%), while CO was higher by more than 80 ppb in October and November in 2006 relative to 2005. The enhancement in CO became smaller in December. TES data suggested less H_2O over Indonesia and the eastern Indian Ocean in 2006 relative to 2005. These differences were caused by large fire emissions from Indonesia in 2006. The anomalously high levels of CO and O_3 over Indonesia in 2006 observed by TES were verified by independent studies of fire emissions. Van der Werf et al. [27] estimated CO emissions of 82 Tg between August and November 2006 (due to large fires in Indonesia), much higher than the amount recorded during the same months in 2004 and 2005, which are 24 Tg and 14 Tg, respectively. Reduction in convection and in photochemical loss of ozone because of lower water vapor also contributed to the ozone enhancement in 2006.

It is expected that summertime circulations associated with the Asian monsoon significantly influence the spatial distribution of ozone and its precursors. However, there have been limited in situ measurements to characterize the distribution of tropospheric ozone and its precursors over the Asian monsoon region. As TES has a great sensitivity to tropospheric ozone in the middle and upper troposphere, it can be used to characterize the horizontal and vertical distribution of tropospheric ozone over this region. Worden et al. [28] focused on TES observations in June, July, and August of 2005 to 2007 and found that there was obvious ozone enhancement over the Middle East and Asia in June and July persistent through the three years, corresponding with the onset period of the Asian summer monsoon. Over the Middle East, ozone levels exceeding 80 ppbv typically occurred between 300 hPa and 450 hPa. Ozone mixing ratios of 150–200 ppbv were observed near 300 hPa over central Asia. The ozone enhancements were found to dissipate in August following the weakening of the summer monsoon. The dynamical and chemical processes responsible for the TES-observed distribution of ozone over Asia are subjects of continuing research. The dynamical process likely involves deep convective transport of ozone and its precursors to the middle and upper troposphere, where the westerly winds in the subtropics and the easterly winds in the tropics will lead to different geographic impacts.

3.3 Future prospective of applications in China

As discussed above, TES data can be used to investigate the horizontal and vertical variations of tropospheric ozone in China. Studies have shown that surface ozone in China exhibits different patterns depending on latitudes and locations. Year-long observations at a rural site (Lin An) near the Yangtze River Delta region in central east China [12], a coastal site (Tai O) near Hong Kong in south China [29] and a rural site (Miyun) near Beijing in North China Plain [11], showed that surface ozone peaked in autumn over southern China, in spring over the Yangtze Delta region, and in early summer over the North China Plain. Current understanding of the factors controlling the temporal and spatial distribution of tropospheric ozone in China is far from complete. Using TES retrievals of tropospheric ozone and CO, one can obtain seasonal variations of the two species over China, which is not limited to the sparsely located surface sites. With the aid of chemical transport models, TES data can provide new insights on the large-scale transport of ozone and CO. Compared with studies over North America and Europe, a disadvantage here is that aircraft and sonde observations carefully designed to validate TES retrievals are not available over China.

It is noticed that tropospheric ozone over China is not only influenced by the Asian monsoon but also by the El Niño phenomenon. Figure 4 presents the monthly mean ozone distributions in July from 2005 to 2007 at 464 hPa, adapted from Worden et al. [28], considering that 2006 was an El Niño year. TES data suggests that the ozone concentrations in 2005 and 2007 were obviously higher than in 2006 over the central Chinese region denoted by the blue rectangular in the figure. It is not clear if and how El Niño will influence tropospheric ozone over China, while it is worthwhile to investigate this feature via TES.

Special observations have been scheduled and may be requested from TES to make geographically focused observations of O_3 and CO over China. From 2008 to 2009, TES made special observations over Beijing and its surrounding regions for the scientific purpose of examining the air quality changes during the 2008 Beijing Olympics relative to the following year. Figure 5 presents the retrieved CO profiles from two Step & Stare special observations over Beijing. One was conducted on August 13, 2008 during the Olympics period and the other on August 16, 2009 after the Olympics. TES revealed reducing CO pollution levels over Beijing during the Olympics as compared to the same period in 2009. The reduction in CO is pronounced at the lower and middle troposphere. TES observations suggested that emission reduction measures implemented during the Olympics were successful in improving air quality over Beijing. Quantitative assessment of the air quality improvement as seen by TES will require chemical transport model simulations in conjunction with the sensitivity analysis of TES retrievals to the a priori and averaging kernels.

4 Discussion and summary

This paper briefly reviews the characteristics of the TES instrument, the retrieval of TES products, and the validation of the TES retrievals of O_3 and CO. As compared to previous satellite instruments, the accurate high spectral resolution measurements made by TES on Aura allow it to survey the middle and lower tropospheric ozone concentrations. It is also the first satellite instrument to provide simultaneous concentrations of carbon monoxide, ozone, water vapor, and methane throughout Earth's lower atmosphere. The applications of TES O_3 and CO products include mapping the vertical and horizontal distribution of tropospheric O_3 and CO and their correlations, examining the regional and continental outflow of O_3 and CO, and analyzing the monthly and annual variation of the two species resulting from certain weather and climatic conditions, such as El Niño and the Asian monsoon. For China, where high quality and routine

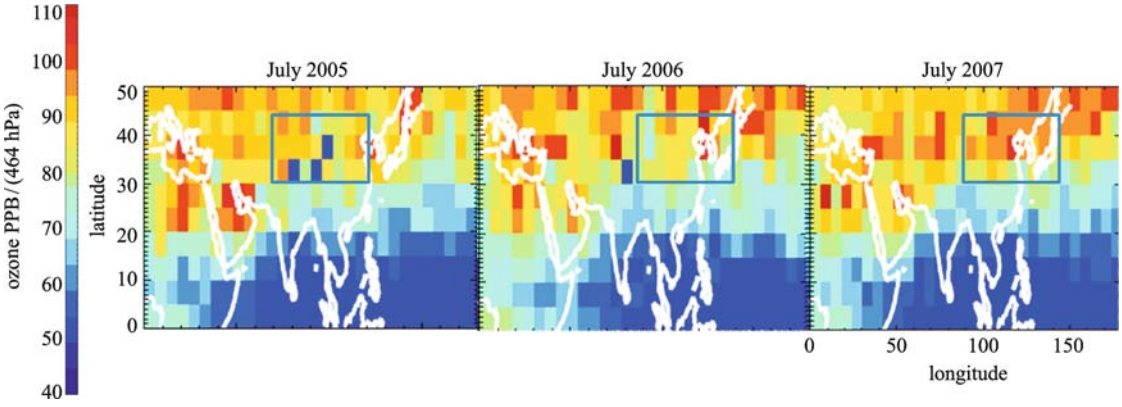

Fig. 4 Monthly averaged ozone mixing ratios retrieved from TES at 464 hPa for Julys of 2005–2007
Notes: Data are gridded onto 6 × 6 bins; figure is adapted from Worden et al. [28]; the blue rectangle denotes the central China region where the ozone variations are discussed in the text

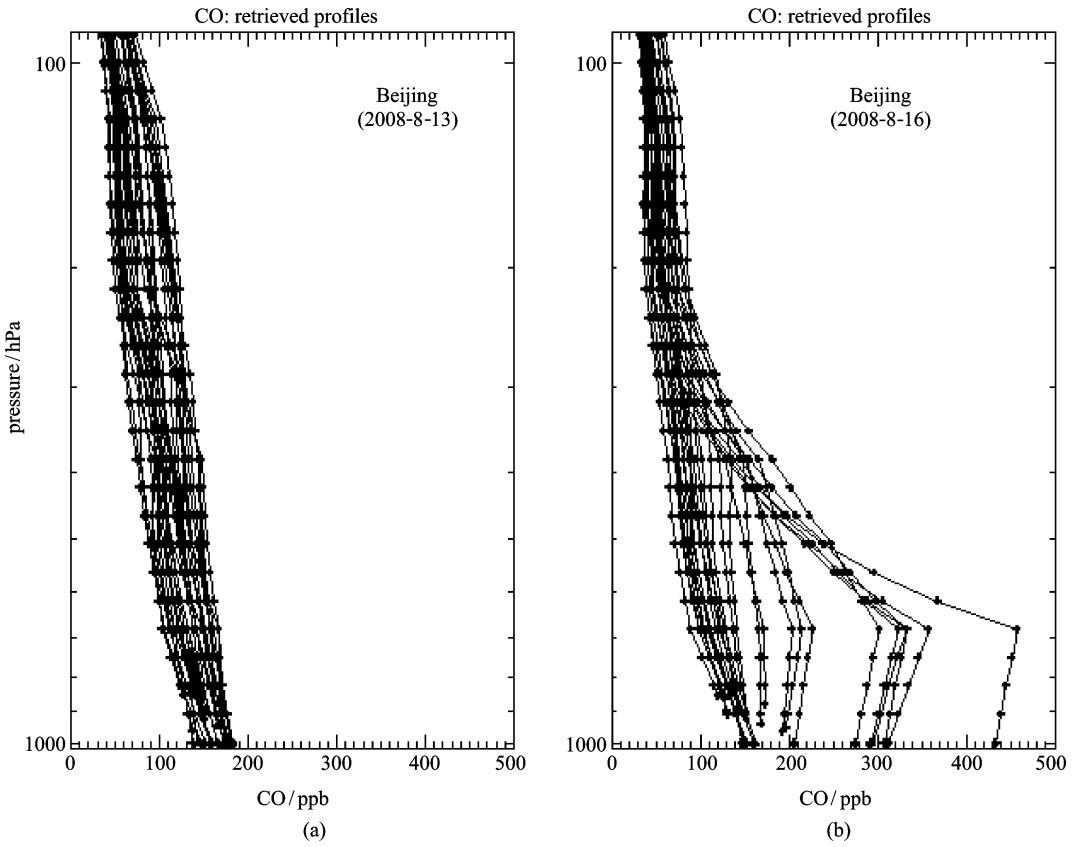

Fig. 5 TES retrieved CO profiles for two transect special observations over Beijing: (a) 13 August 2008; (b) 16 August 2009 (http://tes.jpl.nasa.gov/visualization/l2plots/)

surface measurements of ozone and its precursors are largely absent, TES observations of O_3 and CO provide an important new source of data offering good spatial and temporal coverage. Special observations requests may be submitted to the TES team to make geographically focused observations of O_3 and CO. When used in combination with routine surface measurements of ozone and CO, TES retrievals of tropospheric ozone and CO can provide powerful constraints on the performance of chemical transport models in simulating the general features of ozone over China. Another instrument aboard the Aura satellite, the Ozone Monitoring Instrument (OMI) provides retrievals of NO_2 column densities and aerosol indices that are also useful in air quality studies in conjunction with TES.

Acknowledgements This research was supported by the Program of "Research on Key Technology of Environmental Pollution Control and Quality Improvement" (No. 2007DFC90170). The authors thank Dr. M. Luo at Jet Propulsion Laboratory for helpful discussions and suggestions.

References

1. Brasseur G J J O. Atmospheric Chemistry and Global Change. New York: Oxford Univ Press, 1999: 11–12
2. Staehelin J, Thudium J, Buehler R, Volzthomas A, Graber W. Trends in surface ozone concentrations at arosa (Switzerland). Atmospheric Environment, 1994, 28(1): 75–87
3. Jacob D J, Heikes B G, Fan S M, Logan J A, Mauzerall D L, Bradshaw J D, Singh H B, Gregory G L, Talbot R W, Blake D R, Sachse G W. Origin of ozone and NOx in the tropical troposphere: A photochemical analysis of aircraft observations over the South Atlantic basin. Journal of Geophysical Research-Atmospheres, 1996, 101(D19): 24235–24250
4. Thompson A M, Pickering K E, Mcnamara D P, Schoeberl M R, Hudson R D, Kim J H, Browell E V, Kirchhoff V, Nganga D. Where did tropospheric ozone over southern Africa and the tropical Atlantic come from in October 1992? Insights from TOMS, GTE TRACE A, and SAFARI 1992. Journal of Geophysical Research-Atmospheres, 1996, 101(D19): 24251–24278
5. Fiore A M, Jacob D J, Bey I, Yantosca R M, Field B D, Fusco A C, Wilkinson J G. Background ozone over the United States in summer: Origin, trend, and contribution to pollution episodes. Journal of Geophysical Research-Atmospheres, 2002, 107(D15): 4275
6. Akimoto H, Narita H. Distribution of SO_2, NO_X and CO_2 emissions from fuel combustion and industrial activities in Asia with 1-degrees-X1-degrees resolution. Atmospheric Environment, 1994, 28(2): 213–225
7. Streets D G, Bond T C, Carmichael G R, Fernandes S D, Fu Q, He D, Klimont Z, Nelson S M, Tsai N Y, Wang M Q, Woo J H, Yarber

K F. An inventory of gaseous and primary aerosol emission in Asia in the year 2000. Journal of Geophysical Research, 2003, 108(D21): E30–E31

8. Ding A J, Wang T, Thouret V, Cammas J P, Nedelec P. Tropospheric ozone climatology over Beijing: Analysis of aircraft data from the MOZAIC program. Atmospheric Chemistry and Physics, 2008, 8(1): 1–13
9. Wang T, Wei X L, Ding A J, Poon C N, Lam K S, Li Y S, Chan L Y, Anson M. Increasing surface ozone concentrations in the background atmosphere of Southern China, 1994-2007. Atmospheric Chemistry and Physics, 2009, 9(16): 6216–6226
10. Lin W, Xu X, Zhang X, Tang J. Contributions of pollutants from north china plain to surface ozone at the shangdianzi GAW station. Atmospheric Chemistry and Physics, 2008, 8(19): 5889–5898
11. Wang Y, Mcelroy M B, Munger J W, Hao J, Ma H, Nielsen C P, Chen Y. Variations of O-3 and CO in summertime at a rural site near Beijing. Atmospheric Chemistry and Physics, 2008, 8(21): 6355–6363
12. Wang T, Cheung T F, Li Y S, Yu X M, Blake D R. Emission characteristics of CO, NO_x, SO_2 and indications of biomass burning observed at a rural site in eastern China. Journal of Geophysical Research-Atmospheres, 2002, 107(D12): 4157
13. Bowman K W, Worden J, Steck T, Worden H M, Clough S, Rodgers C. Capturing time and vertical variability of tropospheric ozone: A study using TES nadir retrievals. Journal of Geophysical Research-Atmospheres, 2002, 107(D23): 4723
14. Luo M, Rinsland C P, Rodgers C D, Logan J A, Worden H, Kulawik S, Eldering A, Goldman A, Shephard M W, Gunson M, Lampel M. Comparison of carbon monoxide measurements by TES and MOPITT: influence of a priori data and instrument characteristics on nadir atmospheric species retrievals. Journal of Geophysical Research-Part D-Atmospheres, 2007, 112(D9): D09303
15. Bowman K W, Rodgers C D, Kulawik S S, Worden J, Sarkissian E, Osterman G, Steck T, Lou M, Eldering A, Shephard M, Worden H, Lampel M, Clough S, Brown P, Rinsland C, Gunson M, Beer R. Tropospheric emission spectrometer: Retrieval method and error analysis. IEEE Transactions on Geoscience and Remote Sensing, 2006, 44(5): 1297–1307
16. Rodgers C D. Inverse Methods for Atmospheric Sounding: Theory and Practice. London: World Sci, 2000
17. Brasseur G P, Hauglustaine D A, Walters S, Rasch P J, Muller J F, Granier C, Tie X X. MOZART, a global chemical transport model for ozone and related chemical tracers 1. Model description. Journal of Geophysical Research-Atmospheres, 1998, 103(D21): 28265–28289
18. Nassar R, Logan J A, Worden H M, Megretskaia I A, Bowman K W, Osterman G B, Thompson A M, Tarasick D W, Austin S, Claude H, Dubey M K, Hocking W K, Johnson B J, Joseph E, Merrill J, Morris G A, Newchurch M, Oltmans S J, Posny F, Schmidlin F J, Vomel H, Whiteman D N, Witte J C. Validation of Tropospheric Emission Spectrometer (TES) nadir ozone profiles using ozonesonde measurements. Journal of Geophysical Research-Part D-Atmospheres, 2008, 113(D15): D15S17
19. Osterman G B, Kulawik S S, Worden H M, Richards N A D, Fisher B M, Eldering A, Shephard M W, Froidevaux L, Labow G, Luo M, Herman R L, Bowman K W, Thompson A M. Validation of Tropospheric Emission Spectrometer (TES) measurements of the total, stratospheric, and tropospheric column abundance of ozone. Journal of Geophysical Research-Part D-Atmospheres, 2008, 113 (D15): D15S16
20. Richards N, Osterman G B, Browell E V, Hair J W, Avery M, Li Q B. Validation of Tropospheric Emission Spectrometer ozone profiles with aircraft observations during the intercontinental chemical transport experiment-B. Journal of Geophysical Research-Atmospheres, 2008, 113(D16): D16S29
21. Zhang L, Jacob D J, Bowman K W, Logan J A, Turquety S, Hudman R C, Li Q B, Beer R, Worden H M, Worden J R, Rinsland C P, Kulawik S S, Lampel M C, Shephard M W, Fisher B M, Eldering A, Avery M A. Ozone-CO correlations determined by the TES satellite instrument in continental outflow regions. Geophysical Research Letters, 2006, 33(18): L18804
22. Mauzerall D L, Narita D, Akimoto H, Horowitz L, Walters S, Hauglustaine D A, Brasseur G. Seasonal characteristics of tropospheric ozone production and mixing ratios over East Asia: A global three-dimensional chemical transport model analysis. Journal of Geophysical Research-Atmospheres, 2000, 105(D14): 17895–17910
23. Mauzerall D L, Logan J A, Jacob D J, Anderson B E, Blake D R, Bradshaw J D, Heikes B, Sachse G W, Singh H, Talbot B. Photochemistry in biomass burning plumes and implications for tropospheric ozone over the tropical South Atlantic. Journal of Geophysical Research-Atmospheres, 1998, 103(D7): 8401–8423
24. Parrish D D, Holloway J S, Trainer M, Murphy P C, Forbes G L, Fehsenfeld F C. Export of north-American ozone pollution to the north-Atlantic ocean, Science, 1993, 259(5100): 1436–1439
25. Zhang L, Jacob D J, Boersma K F, Jaffe D A, Olson J R, Bowman K W, Worden J R, Thompson A M, Avery M A, Cohen R C, Dibb J E, Flock F M, Fuelberg H E, Huey L G, Mcmillan W W, Singh H B, Weinheimer A J. Transpacific transport of ozone pollution and the effect of recent Asian emission increases on air quality in North America: An integrated analysis using satellite, aircraft, ozonesonde, and surface observations. Atmospheric Chemistry and Physics, 2008, 8(20): 6117–6136
26. Logan J A, Megretskaia I, Nassar R, Murray L T, Zhang L, Bowman K W, Worden H M, Luo M. Effects of the 2006 El Nino on tropospheric composition as revealed by data from the Tropospheric Emission Spectrometer (TES). Geophysical Research Letters, 2008, 35(3): L03816
27. van der Werf G R, Randerson J T, Giglio L, Collatz G J, Kasibhatla P S, Arellano A F. Interannual variability in global biomass burning emissions from 1997 to 2004. Atmospheric Chemistry and Physics, 2006, 6: 3423–3441
28. Worden J, Jones D, Liu J, Parrington M, Bowman K, Stajner I, Beer R, Jiang J, Thouret V, Kulawik S, Li J, Verma S, Worden H. Observed vertical distribution of tropospheric ozone during the Asian summertime monsoon. Journal of Geophysical Research-Atmospheres, 2009, 114: D13304
29. Wang T, Ding A J, Gao J, Wu W S. Strong ozone production in urban plumes from Beijing, China. Geophysical Research Letters, 2006, 33(21): L21806